A Tumor Promoter Induces Rapid and Coordinated Reorganization of Actin and Vinculin in Cultured Cells

MANFRED SCHLIWA, TAMMIE NAKAMURA, KEITH R. PORTER, and URSULA EUTENEUER

Department of Zoology, University of California, Berkeley, California 94720; and Department of Molecular, Cellular, and Developmental Biology, University of Colorado, Boulder, Colorado 80309. Dr. Porter's present address is the Department of Biological Sciences, University of Maryland, Catonsville, Maryland 21228.

ABSTRACT Treatment of epithelial African green monkey kidney (BSC-1) cells with the potent tumor promoter 12-*O*-tetradecanoylphorbol-13-acetate (TPA) induces a rapid and reversible redistribution of actin and vinculin that is detectable after only 2 min of treatment. Within 20–40 min, stress fibers disappear, while at the same time large actin-containing ribbons resembling ruffles develop both at the cell periphery and in more central regions. Vinculin is associated with these actin ribbons or bands in a punctate or patchy staining pattern. Adhesion to the substratum is changed from predominantly focal contacts associated with stress fiber ends in untreated cells to broad zones of close contact after TPA treatment. High voltage electron microscopic observations disclose the ribbons to consist of highly cross-linked actin filament networks. Thus, an association of vinculin with filament networks, rather than (the ends of) filament bundles, is demonstrated. The integrity of microtubules and vimentin filaments is not affected by TPA treatment, but their distribution is altered to conform with the highly distorted cell shape. The response to TPA is neither prevented nor modified by nocodazole-induced depolymerization or taxol-induced stabilization of microtubules. An intact intermediate filament network seems not required either since colcemid-induced collapse of vimentin filaments towards the nucleus does not affect the cell's response to TPA. Rapid redistribution of actin and vinculin also takes place in enucleated cells and in the presence of cycloheximide, but is prevented by dinitrophenol or oligomycin. TPA-induced cytoskeletal alterations are independent of fibronectin expression and not mimicked, modified, or prevented by calmodulin inhibitors or experimentally elevated levels of calcium and cyclic AMP. Thus the morphological response to TPA involves rapid redistribution of actin and vinculin independent of transcription and translation, fluctuations in the levels of calcium or cyclic AMP, or changes in the organization of microtubules, intermediate filaments, and fibronectin.

Tumor promoters are molecules that are not carcinogenic themselves but that are able to increase the incidence of tumors in tissues pretreated with a carcinogenic agent (for a recent review, see reference 1). The most effective tumor promoter is 12-*O*-tetradecanoylphorbol-13-acetate (TPA [also known as phorbol myristate acetate]),[1] a macrocyclic diterpene ester extracted from the seeds of *Croton tiglium* (2). It has been shown that TPA and related tumor-promoting phorbol esters have profound effects on cultured cells even without pretreatment by a carcinogenic agent. In many respects, these effects resemble those induced by transforming viruses. They include alterations in cell morphology (3), loss of fibronectin from the cell surface (4), stimulation of plasminogen activator production (5), increase in the rate of sugar transport (3), stimulation of cell growth (6), and induction of ornithine decarboxylase (7). Because of the substantial overlap in the activities of tumor promoters and oncogenic viruses (e.g.,

[1] *Abbreviations used in this paper:* PHEM, 60 mM PIPES, 25 mM HEPES, 8 mM EGTA, 2 mM $MgCl_2$; TPA, 12-*O*-tetradecanoylphorbol-13-acetate; BSC-1, African green monkey kidney cells; PtK1, rat kangaroo cells.

THE JOURNAL OF CELL BIOLOGY · VOLUME 99 SEPTEMBER 1984 1045-1059
 · 0021-9525/84/09/1045/15 $1.00

Rous sarcoma virus), it is hoped that the elucidation of the mechanism of action of the tumor promoters may also shed some light on the process of virus-induced transformation.

The precise mechanism of action of tumor promoters is not yet understood. It has been determined that phorbol esters bind to particulate preparations of chick embryo fibroblasts in a specific, saturable manner (8, 9). At least one of these binding sites co-purifies with protein kinase C, the Ca^{++}-activated, phospholipid-dependent protein kinase (10–12). In accordance with this observation, several groups have noted changes in the pattern of protein phosphorylation after treatment with phorbol esters (13–16). However, the role of protein phosphorylation in the cascade of physiological and biochemical changes following treatment of cells with tumor promoters remains to be elucidated.

Tumor promoter-induced changes of the cytoskeleton have not been the subject of intensive research. Many studies just note an "altered morphology" that seems to resemble that of transformed cells (17–20). However, the observed changes in cell morphology were only occasionally studied with respect to specific structural and physiological alterations in the cytoskeleton. Conflicting observations as to the requirement of RNA and protein synthesis (18, 20, 21) or the involvement of plasminogen activator (17, 20) were not resolved.

This study analyzes morphological changes induced by TPA in cultured cells, primarily African green monkey kidney cells (BSC-1), and attempts to determine the cytoskeletal target(s) and effector(s). TPA-induced cytoskeletal changes are extremely rapid, first signs being detectable after only 2 min as a reorganization of filamentous actin and the adhesion plaque protein, vinculin. This reorganization is independent of transcription or translation and microtubule or intermediate filament organization, but dependent on metabolic energy, and is neither mimicked nor prevented by experimental elevation of intracellular calcium or cyclic AMP, or by calmodulin inhibitors. Thus reorganization of actin and vinculin and subsequent changes in cell morphology seem to be brought about by specific events affecting actin and/or the proteins with which it interacts.

MATERIALS AND METHODS

Cell Culture: Several cell types were used in these studies, including African green monkey kidney cells (strain BSC-1), rat kangaroo cells (PtK1), 3T3 fibroblasts, mouse 10T1 cells, and normal rat kidney cells, but this report will be confined to the results obtained with BSC and PtK cells. Qualitatively similar results were obtained with the other cell types employed, even though their response to the various experimental treatments may differ in detail. BSC-1 cells were grown in Dulbecco's modified Eagle medium (Gibco Laboratories, Grand Island, NY) supplemented with 10% fetal calf serum. PtK1 cells (kindly provided by Dr. W. Z. Cande) were grown in F12 medium (Gibco Laboratories).

Immunofluorescence Microscopy: The protocol for fluorescence microscopy used in most of the experiments comprised fixation with 0.5% glutaraldehyde in PHEM (22) buffer (60 mM PIPES, 25 mM HEPES, 8 mM EGTA, 2 mM $MgCl_2$) supplemented with 0.1% Triton X-100 for 10 min (see also reference 23), after which the cells were washed three times with phosphate-buffered saline (PBS). They were then treated with 1% sodium borohydride in PBS (24), washed again, and reacted with either rhodamine phalloidin (25) alone, or a combination of rhodamine phalloidin and an antibody against mammalian tubulin, vinculin, fibronectin (Transformation Research, Inc., Framingham, MA), or vimentin. The cells were washed again, and incubated with the appropriate fluoresceinated second antibodies. Variations of the fixation protocol included glutaraldehyde alone followed by treatment with 0.1% Triton X-100 in PBS, pre-extraction with 0.1% Triton X-100 in PHEM buffer (22) followed by glutaraldehyde fixation, or fixation with 0.15% formalin in PHEM buffer. Essentially the same results were obtained with these fixation schemes. Coverslips were then mounted in 90% glycerol/10% PBS containing 0.1% *p*-phenylene-diamine and viewed in a Zeiss Photomicroscope III.

High Voltage Electron Microscopy: For high voltage electron microscopy, cells were grown on gold grids and processed according to a protocol outlined earlier (22). Briefly, cells were extracted with 0.1% Triton X-100 in PHEM buffer, fixed with 1% glutaraldehyde in PHEM for 10 min, and postfixed with osmium tetroxide (0.5%) for 3 min. Some preparations were reacted with heavy meromyosin-subfragment 1 (kindly provided by Dr. Frank Pepe) before fixation. Preparations were then dehydrated with ethanol, critical point–dried, and viewed in the Boulder high voltage electron microscope at 1,000 kV.

Enucleation: For enucleation, cells were grown on 12-mm round coverslips, inserted cell-side down in a round-bottom centrifuge tube containing culture medium supplemented with 10 μg/ml cytochalasin B, and spun at 12,000 *g* for 40–50 min in a Sorvall centrifuge (DuPont Co., Wilmington, DE). Cytoplasts on coverslips were thoroughly washed with culture medium and used for further experiments within 2–4 h. The enucleation rate usually was 85–95%.

Chemicals: Nocodazole, cycloheximide, dinitrophenol, oligomycin, 2-deoxyglucose, TPA, cytochalasin B, dibutyryl-cyclic AMP, isobutylmethylxanthine, and A23187 were all obtained from Sigma Chemical Co. (St. Louis, MO).

Taxol was a kind gift of Dr. Douros (Natural Products Branch, National Cancer Institute). Trifluoperazine was obtained from Smith, Kline & French, Inc. (Philadelphia, PA). Calmidazolium was a kind gift of Dr. Marc de Brabander (Janssen Pharmaceutica, Beerse, Belgium).

RESULTS

All experiments were performed over a broad time scale ranging from 1 min to 2 d and over a wide range of TPA concentrations (0.1–1,000 ng/ml). For the sake of clarity and brevity, data for the first hour of TPA treatment at a concentration of 50 ng/ml will be presented. It should be mentioned at the outset that the inactive phorbol derivates, 4-α-phorbol and 4-α-phorbol 12,13-didecanoate did not show any of the effects described here for TPA.

Time Course

Treatment of exponentially growing BSC-1 cells with TPA at 50 ng/ml promotes a rapid and dramatic change of their overall morphology (Fig. 1). The normally rounded or polygonal cells adopt an irregular outline with many lamellar, filar, or knobby protrusions at their periphery. In areas of the culture dish in which cells had formed confluent patches, confluency is disrupted and large gaps develop in which the ragged cell peripheries recede from one another. This morphological transformation is completed by 30–40 min and is maintained for as long as the promoter is present.

The organization of actin following TPA treatment was examined by means of fluorescence microscopy using rhodamine-labeled phalloidin which binds specifically to filamentous actin (25). Untreated BSC-1 cells contain a prominent system of filament bundles or stress fibers that are associated with the substrate-apposed cell side (Fig. 2*a*). No prominent staining is revealed in the cell periphery, a finding consistent with the observation that BSC-1 cells possess only relatively small peripheral ruffles (22). Very shortly after TPA is added to the culture medium, changes in actin filament organization are perceived. Within 2 min staining in the cell periphery begins to intensify and so continues for the following 20–40 min, leading to the formation of what appear to be huge ruffles (Fig. 2, *b–f*). In addition, similar actin-containing protuberances of crescent-shaped or circular appearance develop more centrally. With time both the peripheral and central actin whorls become so brilliant that they dominate the fluorescent image and make photographic recording difficult. The process of their formation is surprisingly rapid; many are well developed by 8 min. By 30 min, they are the

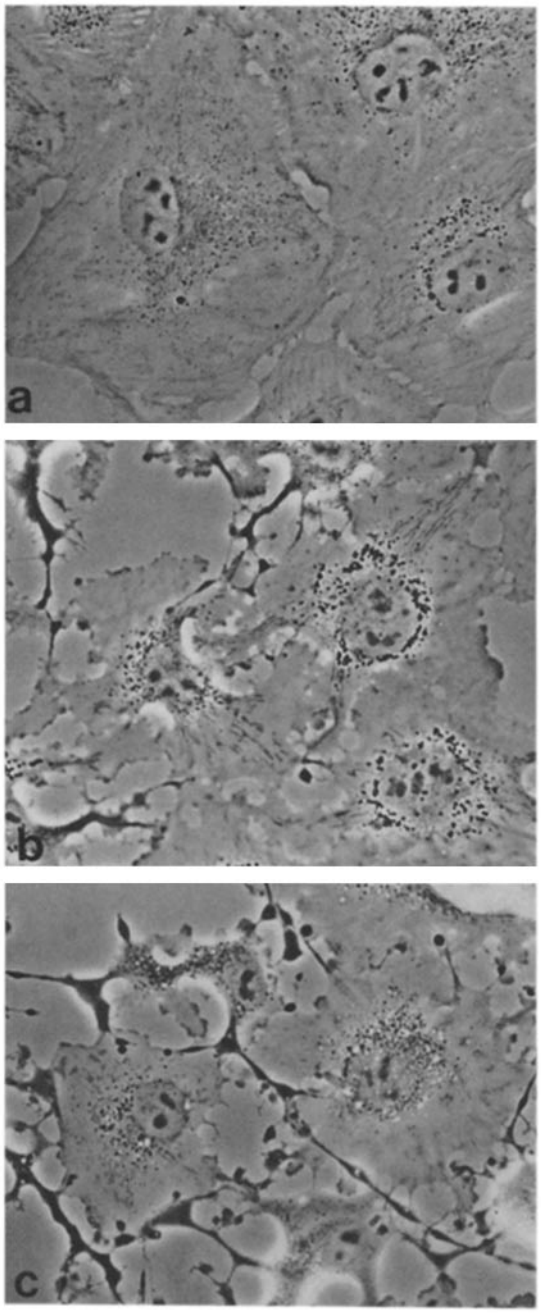

FIGURE 1 Phase-contrast micrographs of BSC-1 cells during TPA treatment. (*a*) Untreated; (*b*) 40 ng/ml TPA for 20 min; (*c*) 40 ng/ml TPA for 40 min. × 400.

single most prominent actin-containing structure of most cells.

While actin whorls are being formed, the stress fiber system disappears. This process is also gradual and overlaps with ruffle formation so that for the first 20–30 min most cells display both structures—the former continually increasing in number and density, the latter waning. Stress fibers disappear in a process of gradual thinning, rather than abrupt breaking or unravelling. Virtually all filament bundles have disappeared by 40–50 min.

The effects of TPA are completely reversible. Recovery proceeds as an almost exact reversion of the original reorganization, only that it takes much longer. Normal cell morphology is restored after 7–10 h.

Correlation with Vinculin Organization

To examine whether this rapid and profound change in actin distribution is accompanied by changes in the organization of vinculin (26, 27), we stained cells with antibodies to mammalian vinculin and rhodamine-phalloidin using standard double-labeling immunofluorescence techniques. As expected, antibody to vinculin intensely stains the ends of stress fibers in untreated cells (Fig. 3*a*). The dimensions of vinculin-containing patches vary considerably, but roughly correlate with the size of the associated stress fibers. Vinculin staining is observed exclusively at the ends of stress fibers; no peripheral staining is evident. TPA treatment leads to a dramatic redistribution of vinculin that is precisely correlated with the redistribution of actin. Vinculin staining after TPA treatment falls into three categories: (*a*) granular, amorphous, or patchy staining associated with peripheral and central actin ruffles, (*b*) staining associated with stress fiber ends, and (*c*) staining of "adhesion junctions."

(*a*) Soon after peripheral or central ruffle-like structures appear, vinculin is found associated with them as faint and rather indistinct accumulations of small patches. These rapidly grow in size, number, and intensity as the actin ribbons grow larger. Only within the first few minutes of TPA treatment are examples of actin-containing ruffles found that apparently do not have any vinculin staining associated with them. Thus, it is possible that, at least in some instances, vinculin associates with pre-formed actin-containing structures. We were unable to find any evidence for the formation of granular vinculin patches before actin associates with them.

(*b*) With respect to vinculin's association with stress fiber ends, there is again a strict correlation. As long as stress fibers persist in TPA-treated cells, and some cells still possess stress fibers after 30–40 min of treatment with TPA, there is vinculin present at their ends. Occasionally stress fiber-associated vinculin patches are found where most of the actin bundle has already disappeared, except for a small patch that co-localizes with the remaining vinculin (Fig. 3, *c* and *d*). The identification of these patches as stress fiber-associated is suggested by their characteristic spearhead shape. Once all stress fibers have disassembled, the vinculin staining formerly associated with their ends also disappears.

(*c*) An unusual staining pattern that is observed in ~10–20% of the TPA-treated cells appears at sites where neighboring cells are in contact. These sites are characterized by a co-localization of actin and vinculin, the former as a band of intense staining, the latter along two parallel lines separated by an unstained gap (Fig. 4*a*). Similar structures in Rous sarcoma virus–transformed cells are termed adhesion junctions by Shriver and Rohrschneider (28), and this term is adopted here. Typically such junctions extend for ~10–30 μm along the cell margins, but occasionally they reach the dimensions of the junction shown in Fig. 4, *a* and *b*. Most interestingly, however, such junctional staining patterns are not only observed between cells, but also within cells in regions where no contact with a neighboring cell exists. Such "self-junctions" may appear as invaginations of a peripheral junction (not shown), or, as in Fig. 4, *c* and *d*, they may be present in the cell center with no connection to the periphery. Characteristically the trilaminar vinculin staining is accompanied by a broad actin ribbon.

All three forms of vinculin staining—stress fiber-associated feet, ruffle-associated patches or ribbons, and adhesion or self-junctions—are found at the substrate-associated cell side, as

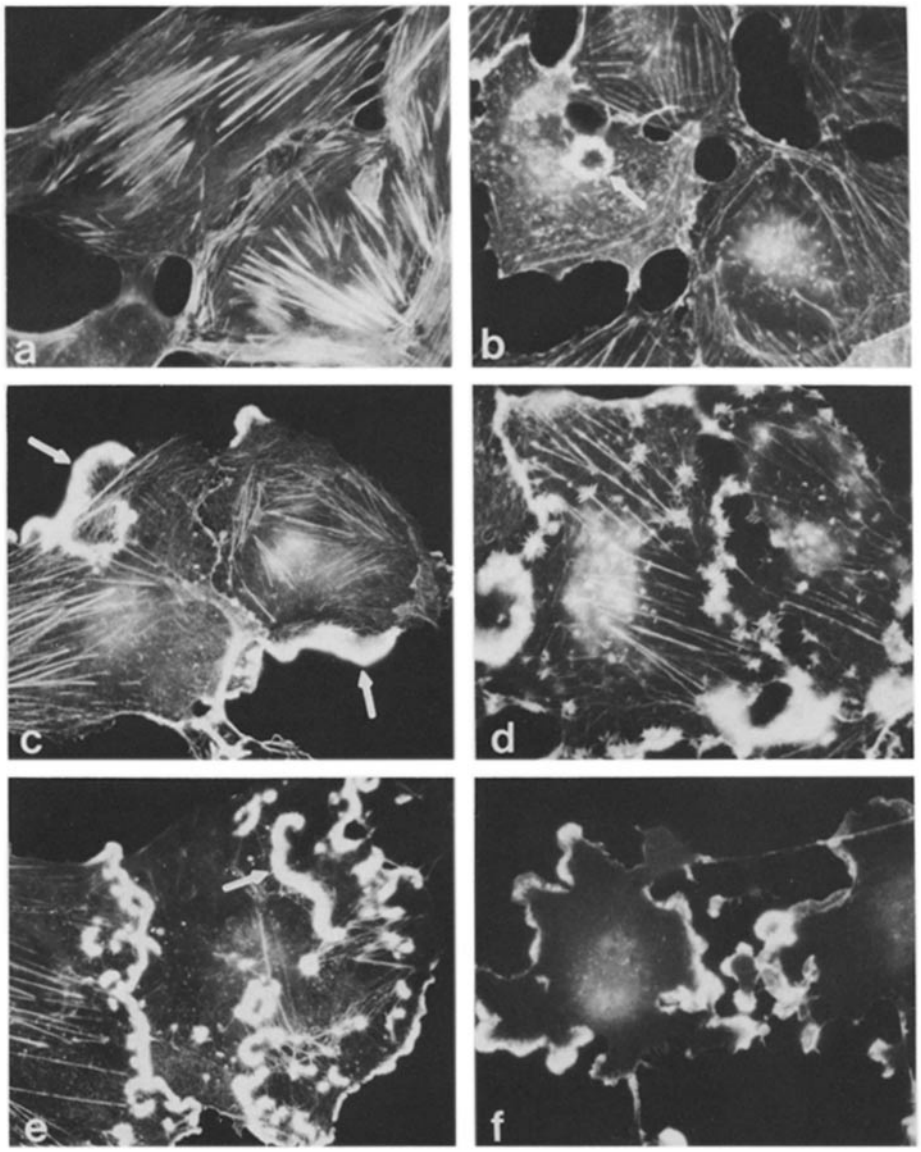

FIGURE 2 BSC-1 cells stained with rhodamin-phalloidin during TPA treatment. (*a*) Untreated. Treatment with 40 ng/ml TPA for 2 min (*b*). 8 min (*c*). 15 min (*d*). 30 min (*e*). 60 min (*f*). × 400.

demonstrated by careful through-focusing. This would mean that both the peripheral and central actin whorls must extend through the thickness of the cell in order for them to maintain an association with vinculin at the substrate face of the membrane. That this is the case is suggested by experiments in which cells are disrupted with a buffer jet that removes the bulk of the cell body and leaves behind only substrate-associated cellular components. As shown in Fig. 4, *e* and *f*, the association of actin with vinculin and of both with the substratum is strong enough to survive this treatment (cf. reference 29).

Substrate Contact

The fact that the modified vinculin staining in TPA-treated cells is found on the substratum-associated cell side (Fig. 4) may suggest a congruence with substrate adhesion zones. To test this, we viewed control and TPA-treated cells with reflection interference-contrast optics (Fig. 5). Whereas stress fibers of untreated cells terminate in dark focal adhesions which, in turn, coincide with vinculin feet, adhesion sites of TPA-treated cells are mostly broad zones of grey close contacts that include, but are not restricted to, the prominent actin and vinculin ribbons. Occasionally, cells are found whose entire ventral surface consists of a close-contact zone, even though ruffles and vinculin ribbons are confined to the cell periphery. Therefore, contact to the substratum is largely uncoupled from the distribution of actin and vinculin after TPA treatment.

High Voltage Electron Microscopy

To determine changes in filament organization at the ultrastructural level, we used high voltage electron microscopy of detergent-extracted whole mount preparations. The transition from an epithelial morphology with a smooth cell outline to a highly distorted cell shape is reflected in the distribution of the cell's filamentous components. Stereo pairs clearly show many of the salient features of the changes in filament organization induced by TPA (Fig. 6). Extensive peripheral networks of very high filament density resembling ruffled regions of other cell types (e.g., neutrophils; see reference 30) dominate the cytoskeleton. The overwhelming majority of the filaments contained in these structures is F-actin, as demonstrated by heavy meromyosin-subfragment 1 decoration. Similar regions of high filament density are found in more central

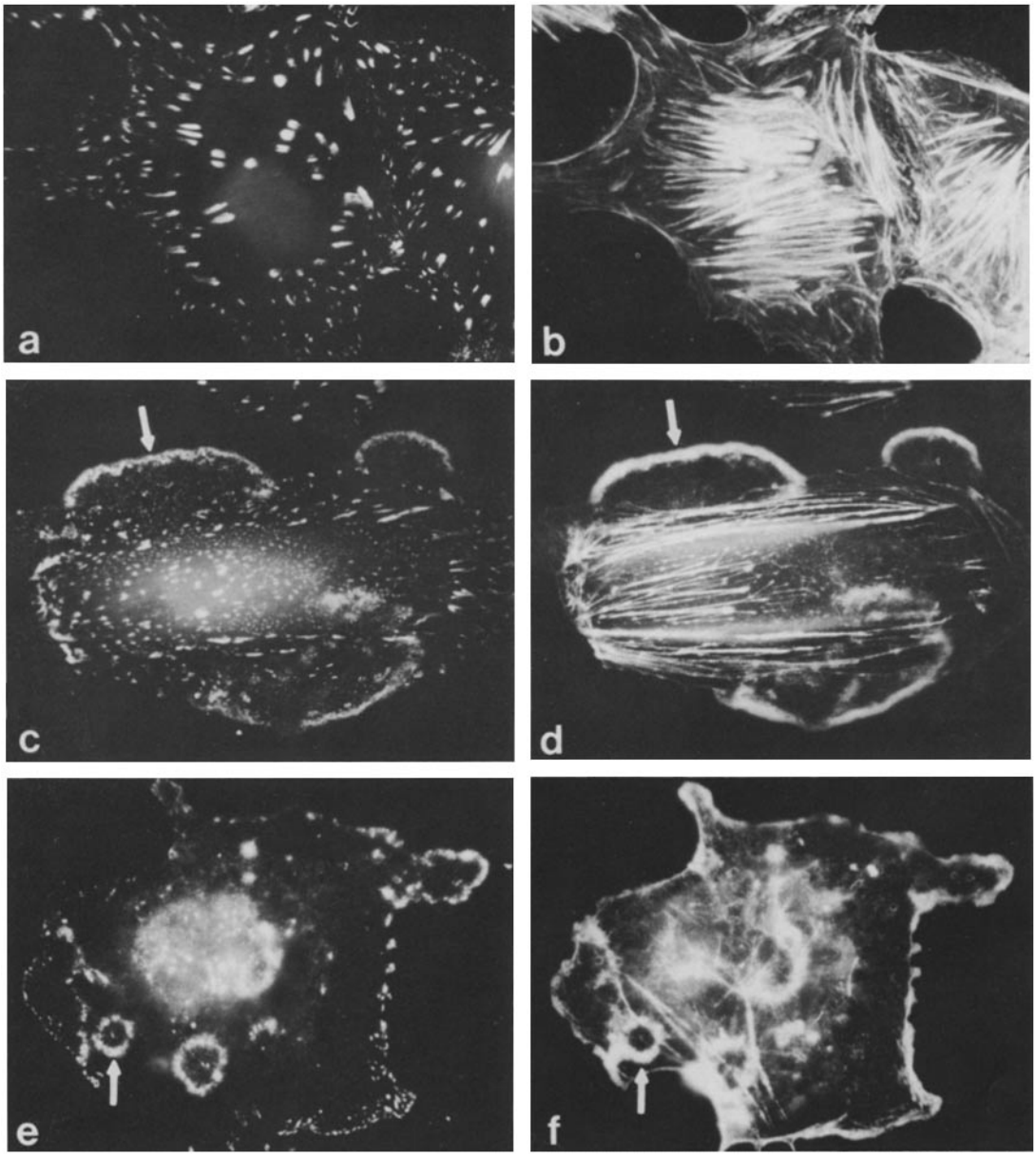

FIGURE 3 BSC-1 cells double-labeled with antibodies against vinculin (*a*, *c*, and *e*) and rhodamin-phalloidin (*b*, *d*, and *f*). (*a* and *b*) Untreated. (*c* and *d*) Treatment with 40 ng/ml TPA for 15 min. (*e* and *f*) Treatment with 40 ng/ml TPA for 30 min. Note appearance of peripheral and central actin ribbons (arrows) in *d* and *f* which are associated with bands of punctate vinculin staining (*c* and *e*), and coexistence of stress fibers and ribbons in *d*. × 400.

cell areas (not shown); in size and shape they clearly resemble the crescent or ring-shaped actin ribbons detected by fluorescence microscopy. Unlike peripheral ruffle-like networks, however, these central filament masses do not protrude extensively from the cell surface.

A second striking feature of TPA cytoskeletons is an overall decrease in filament density throughout most of the cell body except in ruffled networks. Indications of this alteration are easily perceived by comparing the two stereo pairs presented in Fig. 6. Examination of many stereo pairs clearly indicates that this decrease in filament network density is due to a decrease in the number of actin filaments, in agreement with the fluorescence microscopic observations. Coupled with the observation of a high actin filament density in peripheral networks, this suggests that the net result of TPA-induced cytoskeletal rearrangements is a shift of actin filaments from the cell body and stress fibers into cortical networks, with a concomitant loss of normal cell morphology.

Between 15 and 30 min after addition of TPA, when stress fibers are dismantled, many of them are associated with a cloud of filaments near one or both ends (Fig. 7*a*), which give the filament bundle a "bouquet" look. The clouds consist of highly cross-linked networks of actin filaments, as shown by decoration with heavy meromyosin-subfragment 1. Inspection at higher magnification (Fig. 7*b*) reveals the presence of many structural interactions between the major filamentous components of the cytoskeleton (22). Such interactions are mediated by 2–3-nm filament linkers and end-to-side contacts of actin filaments with other actin filaments (Fig. 7*b*), microtubules, and intermediate filaments (not shown). Although quantification is difficult, analysis of many micrographs suggests neither a dramatic increase nor a decrease in

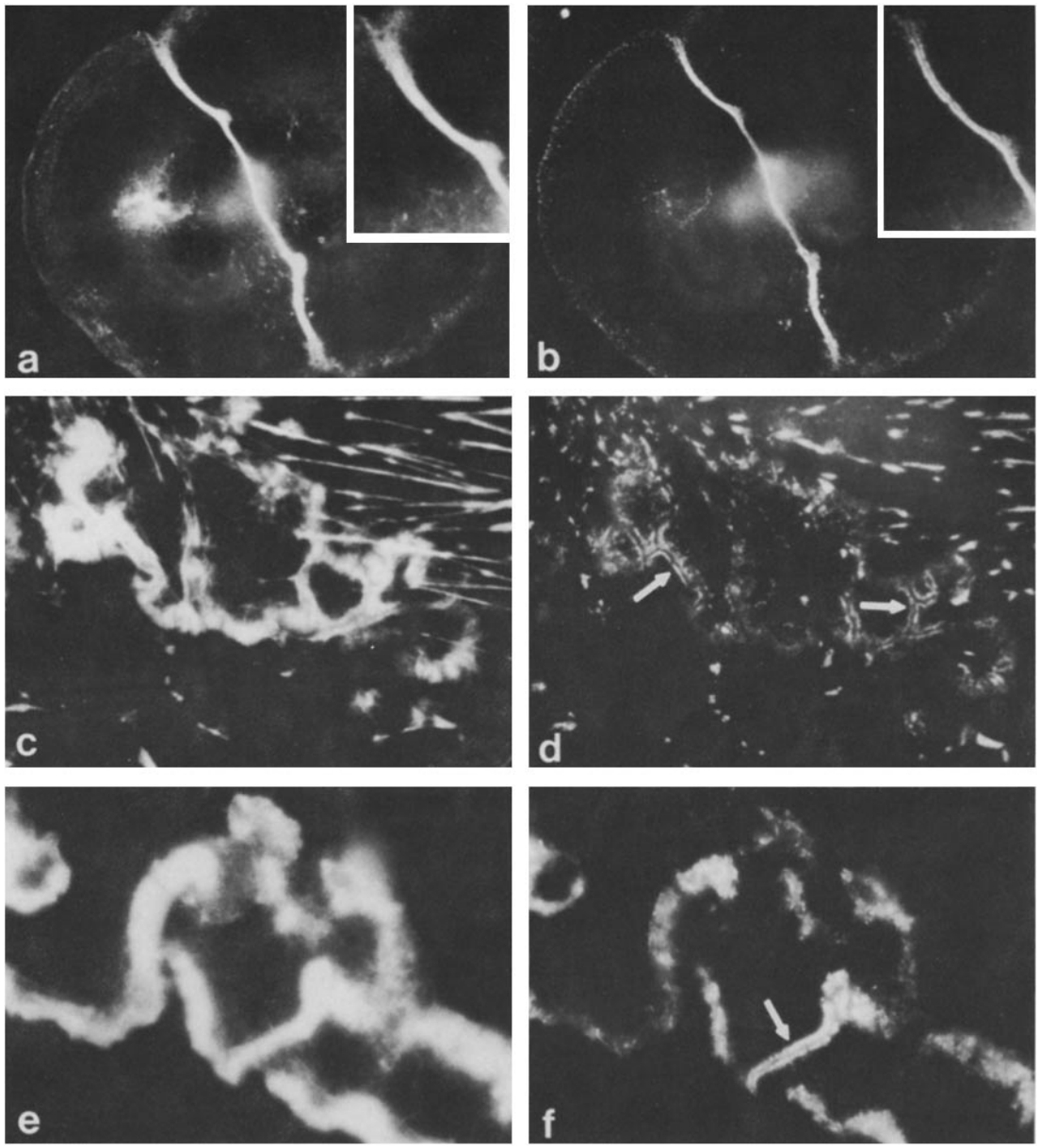

FIGURE 4 (*a* and *b*) Large "adhesion junction" between two neighboring cells stained with rhodamine-phalloidin (*a*) and vinculin (*b*). × 600. (*Insets* to *a* and *b*) Higher magnifications of part of the junctional complex. TPA treatment was for 60 min at 40 ng/ml. × 1,200. (*c* and *d*) Adhesion "self" junctions in the center of a BSC-1 cell, stained with phalloidin in c and vinculin antibodies in *d*. 30-min TPA treatment. Note trilaminar appearance of vinculin staining (arrows). × 1,500. (*e* and *f*) Residues of actin ribbons after the cell body was sheared away with a buffer jet. (*e*) Phalloidin staining, (*f*) Vinculin staining. Note remnant of an "adhesion junction" (arrow). × 1,500.

any of these structural features compared to untreated cells. Rather, their spatial distribution is altered in such a way that they are more abundant in some regions of the cytoskeleton than in others. For example, 2–3-nm filaments are more frequent in the vicinity of dense actin networks (Fig. 7). Outside these areas, actin filaments can be followed for longer distances than in untreated cells, suggesting that the free path length between intersections formed with cross-linking elements is increased.

Microtubules and Intermediate Filaments

A series of experiments was devoted to the question of whether the other two major filamentous components of the cytoskeleton, microtubules and intermediate filaments, are affected by TPA treatment, and to what extent, if at all, they are involved in the morphological TPA response. Double labeling with antibodies against tubulin and rhodamine phalloidin show that the astral microtubule array of untreated cells (see reference 22) is still intact but distorted to conform with the irregular cell shape (Fig. 8, *a–c*). To test whether microtubule integrity or assembly/disassembly are required for TPA-induced cytoskeletal reorganization, we exposed cells to nocodazole (2 μg/ml for 1–2 h) or taxol (4 μg/ml for 6–20 h). While the former compound rapidly depolymerizes microtubules, the latter promotes microtubule assembly and leads to the formation of stable, occasionally bizarre, microtubule arrays throughout the cell body (31–33). Neither of the two drugs significantly affects actin or vinculin organization and

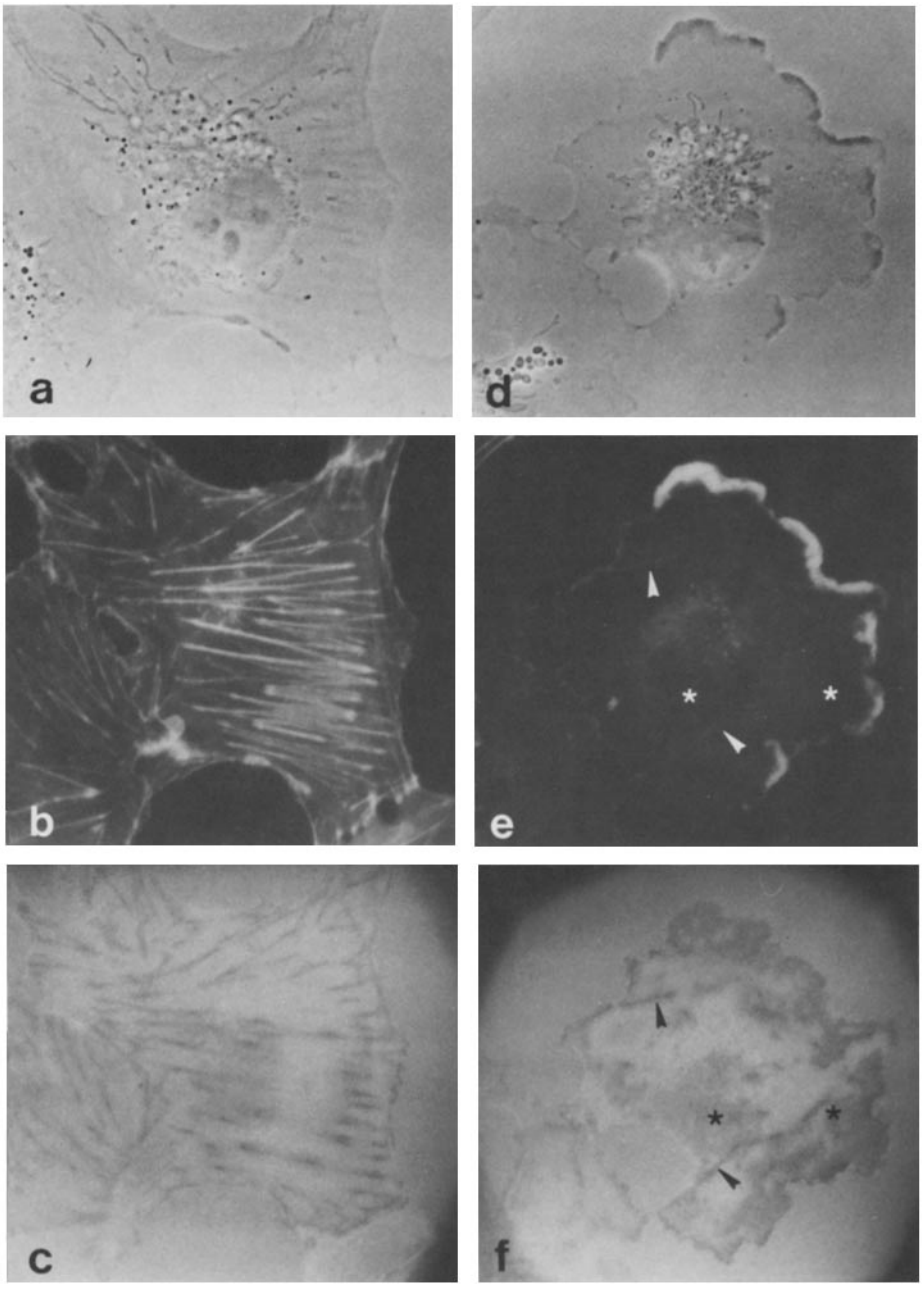

FIGURE 5 Phase-contrast (*a* and *d*), rhodamine-phalloidin staining (*b* and e), and reflection interference-contrast microscopy (c and *f*) of an untreated (*a–c*) BSC-1 cell and a cell treated with 40 ng/ml TPA for 30 min (*d–f*). Dark strands of focal adhesions associated with the ends of stress fibers in control cells are replaced by extensive zones of gray mottled appearance indicative of close contacts. These gray areas include, but are not restricted to (see areas marked by asterisks in e and *f*), the peripheral ribbons of staining to which actin and vinculin are confined. Arrowheads indicate streaks of black focal contacts associated with remnants of filament bundles. × 400.

cell shape; only prolonged treatment (>15 h) leads to a slight decrease in the number of stress fibers. When nocodazole or taxol-treated cells are exposed to TPA, both the time course and the final state of actin and vinculin reorganization are identical to that of cells treated with TPA alone (Fig. 8, *d–f* and *g–i*). Thus these experiments do not suggest a direct involvement of microtubules in TPA-induced morphological transformations.

Like microtubules, BSC-1 intermediate filaments, which are of the vimentin type (22), remain intact after TPA treatment (not shown). Their possible involvement is more difficult to assess, since no experimental treatment is known that selectively affects this filament class. However, by treating live cells with microtubule inhibitors for longer time periods, it is at least possible to influence their distribution within the cell. If BSC-1 cells are kept in the presence of 2 μg/ml nocodazole for 24 h, intermediate filaments collapse towards the cell center and coil up in the vicinity of the nucleus while the cells still maintain a spread epithelial morphology. Subsequent treatment with TPA promotes the same characteristic actin and vinculin reorganization as in control cells (Fig. 9), arguing against the involvement of an intact intermediate filament network in this response.

Fibronectin

Tumor promoters induce loss of fibronectin from the cell surface (4). Since cytoskeleton and cell shape are influenced by the level of fibronectin (34), an obvious question to ask is whether the alterations in actin and vinculin organization observed here are related to, or even induced by, changes in surface-associated fibronectin. Using an antibody directed against fibronectin, very little fibronectin was found to be associated with BSC-1 cells, in agreement with an earlier report (35). Thus, changes in fibronectin organization are not

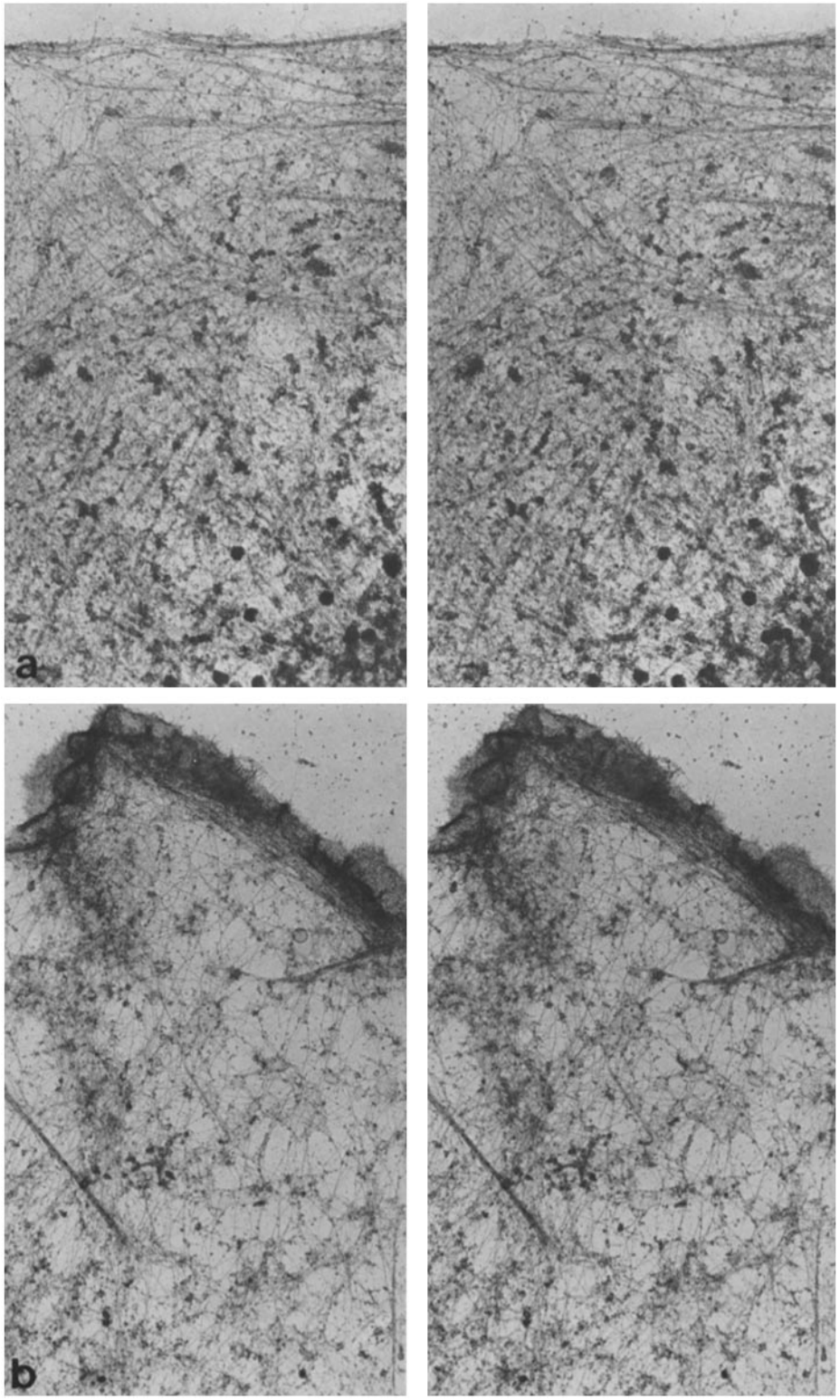

FIGURE 6 Stereo pairs of detergent-extracted control cell (*a*) and a cell treated with TPA for 30 min (*b*). A peripheral region most probably corresponding to an actin ribbon is disclosed as a dense filament network with a ruffle-like appearance. The residual fiber network throughout the cell body appear significantly more open than in control cells. × 5,000.

involved in the morphological TPA response of BSC-1 cells. To test whether fibronectin changes might occur in a cell type that expresses this surface glycoprotein, we used PtK1 cells which lay down a dense fibronectin carpet (Fig. 10, *a* and *b*). Exposure of PtK1 cells to TPA at the same concentration used in BSC-1 cells induces a similar series of dramatic cytoskeletal changes that affect both actin and vinculin (Fig. 10, *e* and *f*), but not the overall organization of fibronectin (Fig. 10, *c* and *d*). However. we cannot exclude the possibility that fibronectin fibers located at, and closely associated with, the cell surface might be altered.

Transcription, Translation, and Metabolic Energy

In agreement with an earlier report (21) that demonstrates that TPA does not require the nucleus to induce morphological changes as seen by phase-contrast microscopy, we find that enucleated BSC-1 cells undergo the same series of changes in actin and vinculin organization over the same time period

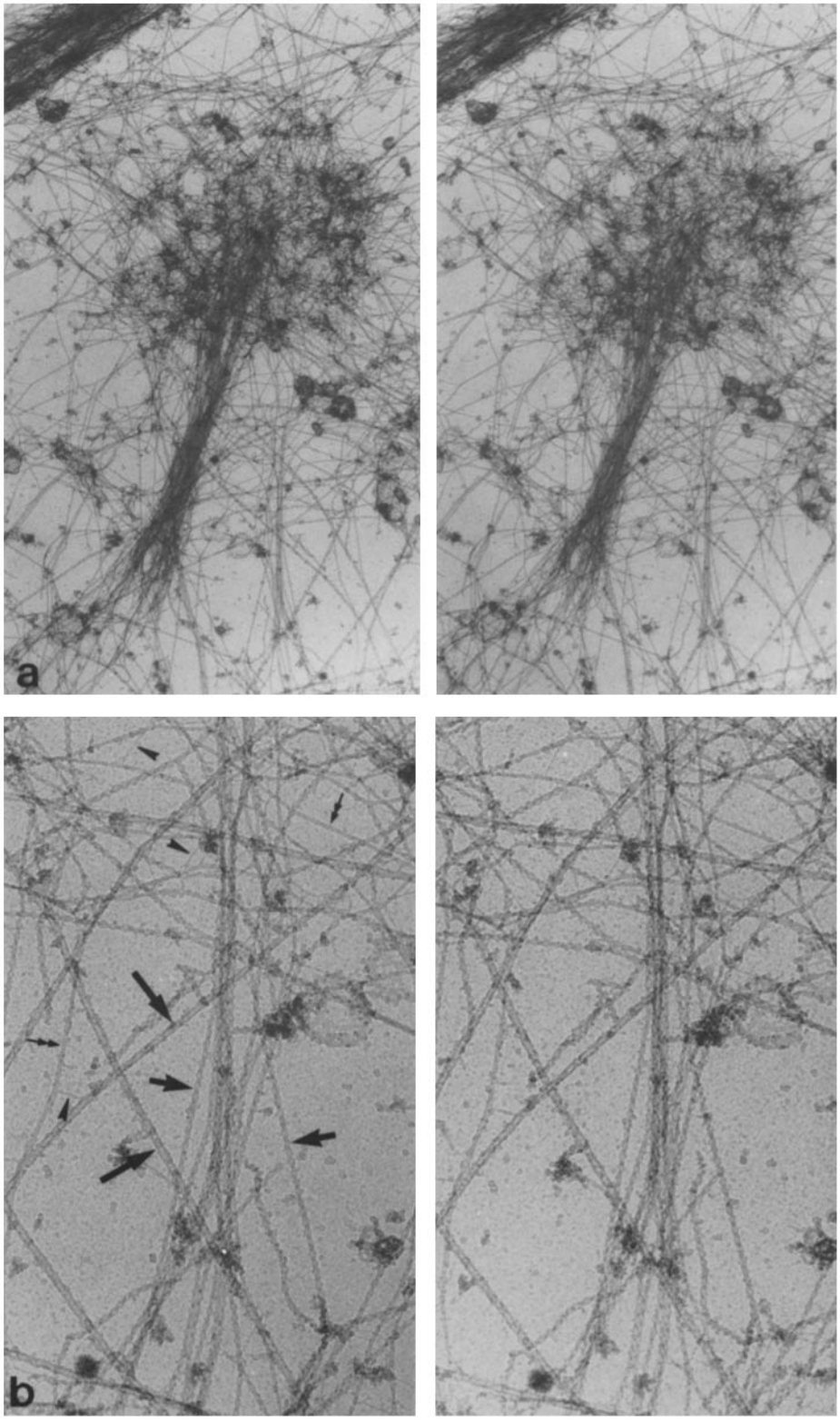

FIGURE 7 Stereo pairs of part of a BSC-1 cell treated with TPA for 20 min. The short filament bundle in *a*, probably a remnant of a stress fiber, is associated with a dense filament network composed mainly of actin filaments. This preparation was decorated with heavy meromyosin-subfragment 1 before fixation. × 18,000. (*b*) higher magnification of part of *a*, demonstrating the presence of all major filamentous components, including microtubules (large arrows), heavy meromyosin-subfragment 1-labeled actin filaments (small arrows), intermediate filaments (double arrows), and 2–3 nm filament linkers (arrowheads). × 68,000.

as intact cells (not shown). Similarly, pretreatment of either intact or enucleated cells with the protein synthesis inhibitor, cycloheximide (10 μg/ml for 1 h), followed by TPA in the presence of the inhibitor, fails to inhibit the reorganization of actin and vinculin. In contrast, pretreatment with dinitrophenol (0.5 mg/ml) or oligomycin (1 μg/ml) in the presence of 2-deoxyglucose (1 mg/ml) in glucose-free medium completely blocks morphological changes and actin or vinculin reorganization (not shown). From these experiments we conclude that TPA-induced morphological changes occur independent of transcription and translation, but require metabolic energy.

Cyclic AMP, Calcium, and Calmodulin

Tumor promoters have been shown to influence cAMP levels and metabolism (e.g., references 36, 37); other studies

link tumor promoters to calcium fluxes (e.g., references 38–41) and calmodulin (e.g., references 42, 43). Both cAMP and calcium play a basic role in cellular metabolism, particularly with respect to protein phosphorylation, and at least some of the effects of TPA on cells may involve changes in phosphorylation (12–15). While studies on cytoskeleton-related

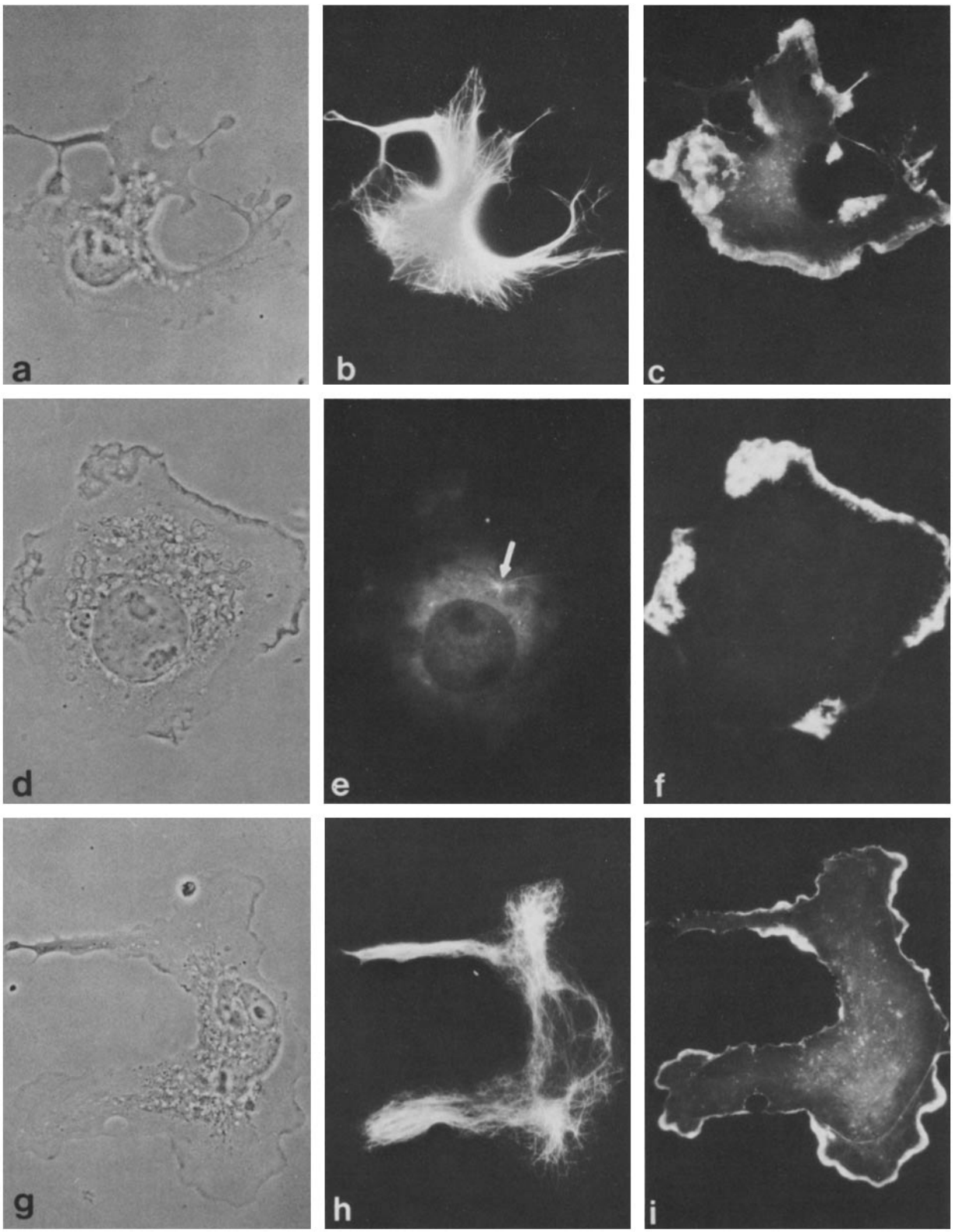

FIGURE 8 Microtubules in TPA-treated BSC-1 cells. Phase contrast (*a*, *d*, and *g*), staining with antibody against tubulin (*b*, *e*, and *h*), and rhodamin-phalloidin (*c*, *f*, and *i*). (*a–c*) 40 min TPA alone. (*d–f*) Pretreatment with 2 μg/ml nocodazole for 1.2 h, followed by TPA treatment in the presence of the drug. Most microtubules are depolymerized, except for a few presumably associated with the centrosome (arrow). (*g–i*) Pretreatment with 4 μg/ml taxol for 15 h, followed by TPA treatment in the presence of the drug. The radial microtubule array is replaced by tufts and networks of microtubule pieces. × 400.

changes in phosphorylation induced by TPA are still under way, we have sought to clarify whether changes in cAMP and calcium levels can enhance, mimick, or inhibit TPA-induced cytoskeletal alterations.

BSC-1 cells treated with 1 mM dibutyryl-cAMP for 6–20 h in the presence of isobutyl methylxanthine, a phosphodiesterase inhibitor, show minor changes in overall cell morphology, including a slightly more irregular outline and condensed and branched stress fibers (Fig. 11 *a*). Vinculin is characteristically concentrated at stress fiber ends (Fig. 11 *b*). However, cAMP/isobutyl methylxanthine pretreatment completely fails to inhibit or modify the series of changes in both actin and vinculin organization induced by TPA (Fig. 11, *c* and *d*). In a similar set of experiments, cells were exposed to the calmodulin inhibitors, calmidazolium (2.5 and 5 μM) or trifluoperazine (10 and 40 μM), for 1–3 h at concentrations known effectively to inhibit calmodulin (44, 45). While causing minor changes in actin organization when used alone (stress fibers are more abundant and appear "frizzy;" see Fig. 12 *a*), the typical response to TPA is not inhibited (Fig. 12, *b* and *c*). In another set of experiments, the calcium ionophore A23187 (2.5 μg/ml for 2–7 h, with 1 mM calcium added to the culture medium), while promoting minor changes in stress fiber organization when used alone (Fig. 12 *d*), does not inhibit or enhance TPA-induced stress fiber dissolution, formation of actin ribbons, and reorganization of vinculin (Fig. 12, *e* and *f*).

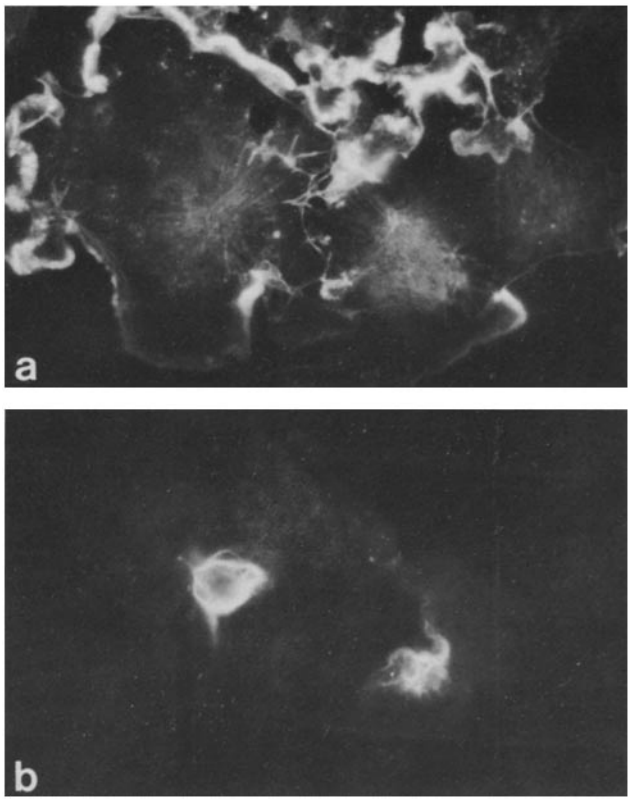

FIGURE 9 Cell treated with 2 μg/ml nocodazole for 24 h, followed by TPA for 40 min. Double labeling was with rhodamine-phalloidin (*a*) and an antibody against vimentin (*b*). Despite collapse of intermediate filaments towards the nucleus, the characteristic actin rearrangement still occurs. × 400.

DISCUSSION

We have analyzed the changes induced by a potent tumor promoter in the organization of the three major filament systems and the adhesion plaque protein, vinculin. TPA promotes a rapid and reversible reorganization of actin and vinculin. The integrity of microtubules and intermediate filaments is not affected, even though their distribution changes to conform with the highly distorted cell shape. In speed of action and the degree of distortion of cellular morphology, these cytoskeletal changes are comparable to those induced by the cytochalasins (46–48). In contrast to previous suggestions, we find that TPA-induced cytoskeletal rearrangements are independent of intact microtubule and intermediate filament networks since they are not prevented by nocodazole depolymerization or taxol stabilization of microtubules, or nocodazole-induced collapse of intermediate filaments. A direct involvement of either microtubules or intermediate filaments therefore seems unlikely.

Contrary to the findings of one group (18), but in agreement with reports by others (20, 21), transcription and translation are not required for the morphological response. Thus changes in the pattern of protein synthesis reported to occur after administration of TPA (e.g., references 5, 7, 13, 49–51), including that of cytoskeletal proteins (52), are unrelated to the morphological events studied here. However, the change in morphology is actively induced by the cell since it is suppressed by inhibitors of energy metabolism.

The rapid and dramatic reorganization of actin and vinculin occurs in a highly coordinated fashion and involves two seemingly independent but overlapping processes: (*a*) dismantling of stress fibers and associated adhesion plaques, and (*b*) development of actin networks with newly-formed vinculin ribbons. The light microscopic appearance of the new vinculin sites is distinctly different from that of plaques at stress fiber ends in that it is punctate, dotted, or diffuse, rather than triangular and sharply delineated. The appearance of the new sites is reminiscent of the vinculin patches or rosettes in Rous sarcoma virus–transformed cells (28, 53, 54). A relationship to the transient vinculin "belts" in EGTA-treated Madin-Darby canine kidney cells (55) may also exist. Thus a change in the organization of vinculin is an additional feature that TPA shares with transforming viruses. Yet another correspondence between the effects of tumor promoters and transforming viruses concerns the induction of "adhesion junctions" that contain actin and vinculin and, in Rous sarcoma virus–transformed cells, the product of the transforming gene, pp60 src (28). Such junctions typically display vinculin staining in two parallel bands separated by an unstained cleft (Fig. 3 *b*). It is interesting that staining with similar characteristics is found not only between cells, but also within cells, in an appearance analogous to that of intracellular or "self"-junctions described for certain pathological conditions or specialized tissues (e.g., references 56, 57). As in peripheral vinculin ribbons, actin is associated with these self-junctions as well.

The co-distribution of vinculin and actin-containing ruffle-like cellular domains represents a novel and unusual form of association between these two cytoskeletal components. To our knowledge, vinculin patches underlying ruffled membrane regions have not been noted in any other cell type. Coupled with the high voltage electron microscopic observation that TPA-induced actin ribbons consist of extensive three-dimensional networks of actin filaments, this constitutes the first observation of vinculin association with actin networks, rather than (the ends of) actin bundles. This form of

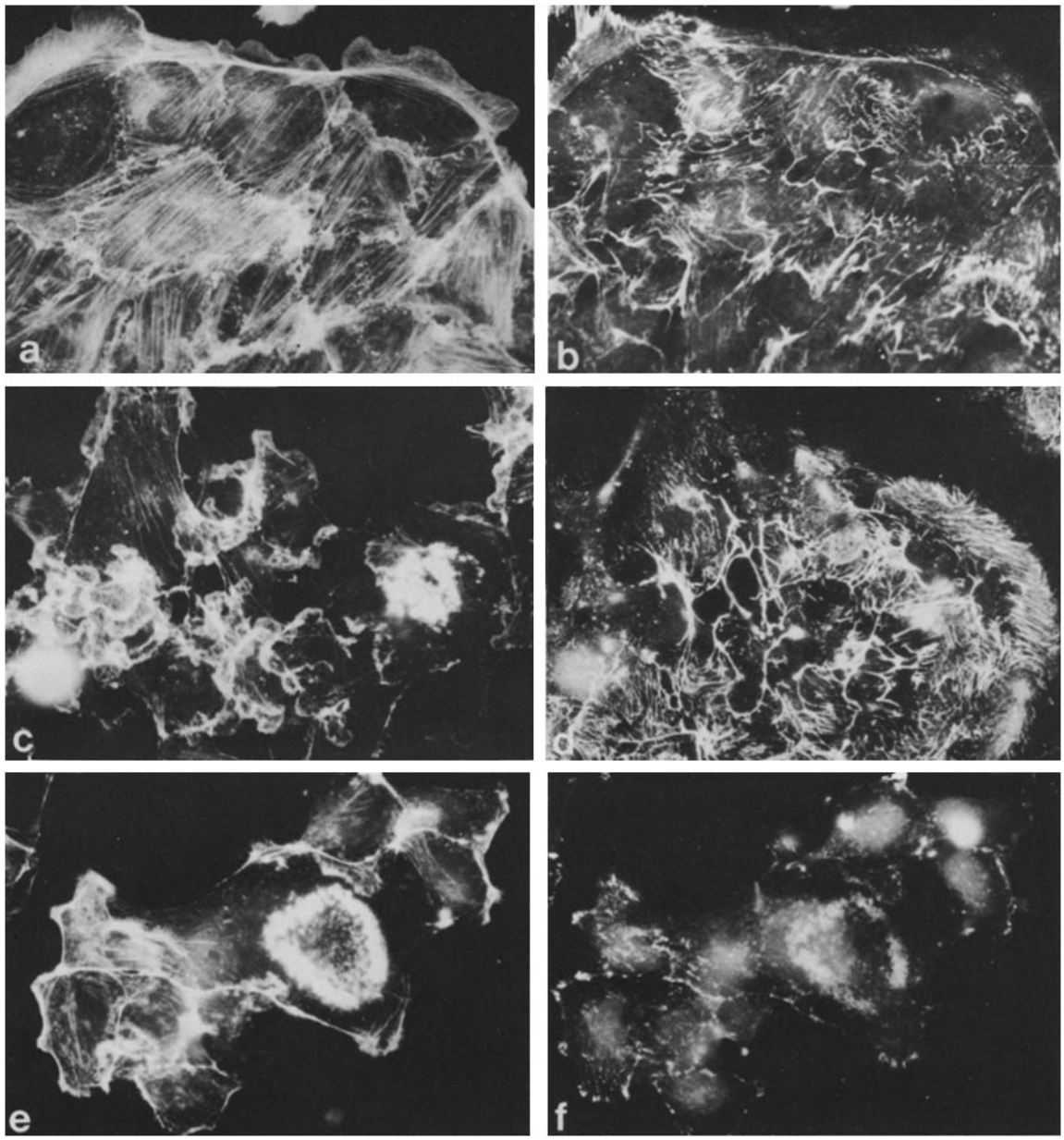

FIGURE 10 PtK_1 cells stained with rhodamine-phalloidin (*a*, *c*, and *e*), antibodies against fibronectin (*b* and *d*), and antibodies against vinculin (*f*). Untreated cells exhibit a prominent system of stress fibers traversing the cells (*a*) and a thick carpet of substrate-associated fibronectin (*b*). TPA treatment at 40 ng/ml for 40 min induces a dramatic reorganization of actin (c), but no apparent change in fibronectin (*d*). Note how the fibronectin carpet in (*d*) still seems to reflect the morphology and organization of the cells before TPA treatment, but now distorted in response to the compound (c). The reorganization of actin in PtK_1 cells induced by TPA is accompanied by a corresponding change in the distribution of vinculin (e and *f*). Note the correspondence of a central actin ring (e) with a similar ring of punctate and patchy vinculin staining (*f*). × 400.

association is consistent with in vitro observations of low affinity binding sites for vinculin along actin filaments, in addition to high affinity sites believed to be localized at the growing filament ends (58, 59). However, the in vitro association of vinculin along the length of actin filaments leads to the formation of actin bundles, rather than three-dimensional networks (59, 60). Therefore, the precise mode of interaction between vinculin and actin within TPA-induced networks observed here requires further study.

A question of particular interest concerns the temporal relationship between the redistribution of actin and the reorganization of vinculin. On the basis of the characteristic association of vinculin with the termini of stress fibers and the congruence of these termini with adhesion plaques, it is tempting to speculate that perturbance of vinculin organization might be related to both the dissolution of stress fibers and the loss of adhesive properties, two prominent features of transformed cells. With respect to stress fiber dissolution, this proposal might also be extended to TPA-treated cells. If it were possible to demonstrate that vinculin reorganization precedes actin redistribution, it would be entirely consistent with this proposal and would constitute strong indirect evidence in its favor. However, careful analysis of our time course studies on double-labeled cells does not corroborate

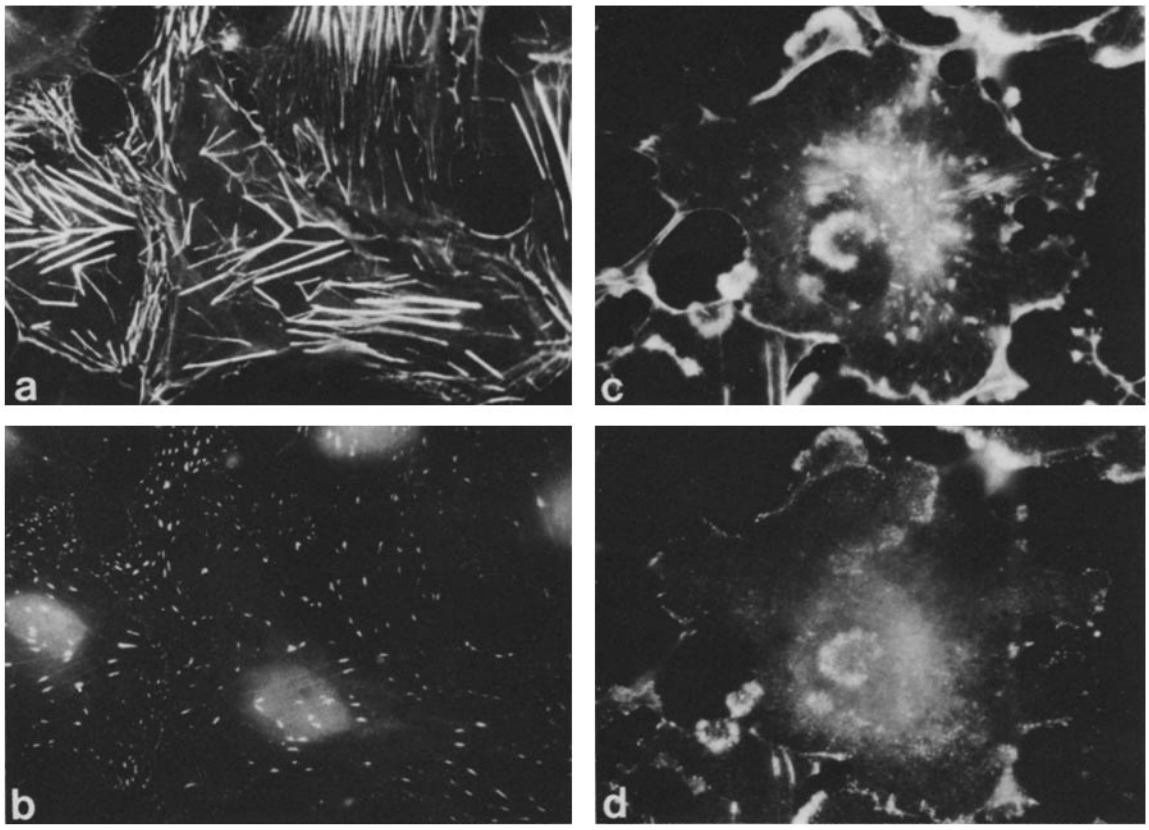

FIGURE 11 BSC-1 cells treated with 1 mM dibutyryl cAMP plus 1 mM isobutylmethylxanthine for 20 h. While causing a minor but clearly perceptible distortion of normal cell morphology and stress fiber organization (*a*), this treatment does not affect the characteristic association of vinculin with stress fiber ends (*b*). In contrast, subsequent treatment with TPA for 40 min still induces the rapid, dramatic rearrangements of both actin (*c*) and vinculin (*d*). × 400.

this view. Vinculin is present at the termini of stress fibers up to the point of their dissolution; in fact, if anything, vinculin plaques are the last to go (Fig. 3, *c* and *d*). Conversely, the formation of TPA-induced vinculin patches and ribbons has not been found to precede the development of actin networks; again, at early time points the reverse is more likely. Thus, on a time scale of minutes or even seconds, actin ribbons and stress fibers are not found without corresponding vinculin patches. The view that changes in vinculin plaques precede actin changes (29, 61) or that vinculin serves as organization sites for the formation of actin bundles (62) is not supported by these experiments. It needs to be considered, however, that vinculin within adhesion plaques might be altered in more subtle ways, leading to effects on actin organization without, at first, corresponding changes in vinculin localization.

What might be the nature of the alterations that affect vinculin? Vinculin is a phosphoprotein with phosphorylation sites at serine, threonine, and tyrosine (63). Accordingly, the level of phosphorylation was considered as a possible regulatory event. This view was strengthened by the observation that in transformed cells, vinculin is "overphosphorylated" at tyrosine (64), and that this biochemical change is accompanied by loss of adhesion plaques (53, 54). However, tyrosine phosphorylation as an event leading to stress fiber dissolution has later been questioned on the basis of experiments with partial transformation mutants of Rous sarcoma virus that induce tyrosine phosphorylation but allow cells to retain stress fibers terminating in vinculin plaques (65). Further, phosphotyrosine is not increased before mitosis when cells dismantle stress fibers (66). On the other hand, vinculin has recently been shown in vitro to be a substrate for protein kinase C, the phospholipid-dependent kinase specific for serine and threonine residues (63). This finding is of particular interest since protein kinase C has been shown to be activated by TPA (12, 67, 68; however, see also reference 16). While studies on possible changes in phosphorylation of cytoskeletal proteins after TPA treatment did not yet yield conclusive results, we show here that cytoskeletal alterations are neither prevented nor mimicked by calmodulin inhibitors or elevated calcium or cAMP, factors known to be involved in phosphorylation-dependent activation of cellular functions. Thus, whether a single-step event involving altered phosphorylation of vinculin can explain the changes in vinculin and actin distribution observed here remains to be demonstrated. These changes are of dual nature, involving dissociation of actin and vinculin in preexisting plaques and a new form of association in ribbons. Whether vinculin in these newly-formed sites possesses altered properties requires further study.

We thank Drs. Larry Rohrschneider, Marc Kirschner, and Fernando Cabral for generously providing antibodies, Dr. Theodor Wieland for a gift of rhodamine-phalloidin, Dr. Douros for a gift of taxol, and Dr. Marc de Brabander for a gift of calmidazolium. We also thank Drs. Roger Pedersen and Zena Werb for allowing the use of their reflection interference-contrast microscope equipment.

This study was supported by a grant from the Cancer Research Coordinating Committee of the University of California to Manfred Schliwa and by Biotechnology Research Resources Program grant

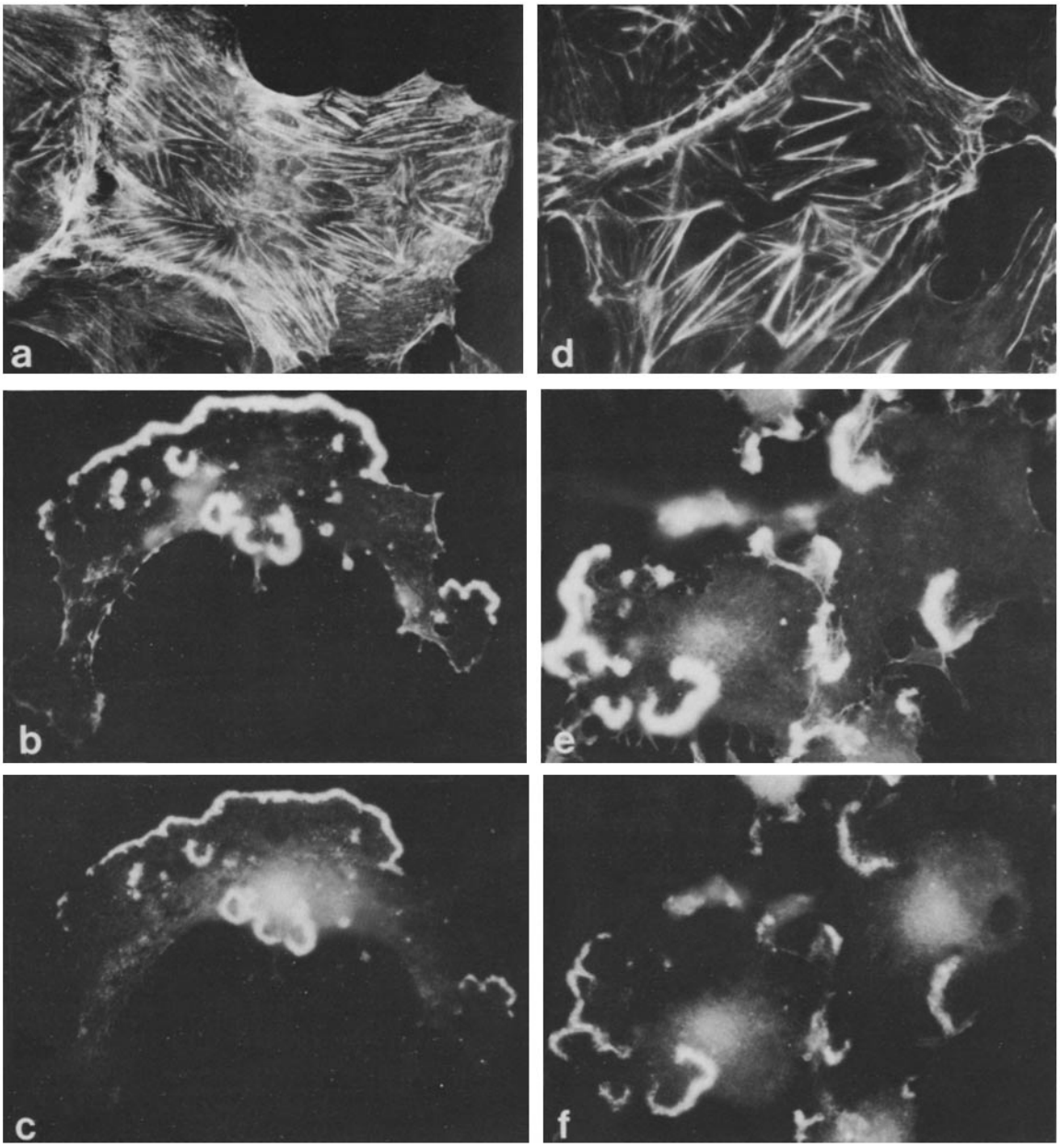

FIGURE 12 BSC-1 cells treated with 5 μM calmidazolium for 2 h (*a–c*) or the ionophore A23187 at 2.5 μg/ml for 5 h (*d–f*). Both compounds induce a change in the organization of stress fibers (*a* and *d*), but neither prevent nor alter nor delay the response to subsequent treatment with TPA for 40 min, both with respect to the organization of actin (*b* and *e*) and vinculin (*c* and *f*). × 400.

RR 00592 fromn the Division of Research Resources, National Institutes of Health to Keith R. Porter.

Received for publication 6 February 1984, and in revised form 8 May 1984.

REFERENCES

1. Blumberg, P. M. 1980. In vitro studies on the mode of action of the phorbol esters, potent tumor promoters. *CRC Crit. Rev. Toxicol.* 8:153–197.
2. Hecker, E. 1968. Carcinogenic principles from the seed oil of *Croton tiglium* and other euphrobiaceae. *Cancer Res.* 28:2338–2349.
3. Driedger, P. E., and P. M. Blumberg. 1977. The effect of phorbol diesters on chicken embryo fibroblasts. *Cancer Res.* 37:3257–3265.
4. Blumberg, P. M., P. E. Driedger, and P. W. Rossow. 1976. Effect of a phorbol ester on a transformation-sensitive surface protein of chick fibroblasts. *Nature* (*Lond.*). 264:446–447.
5. Wigler, M., and I. B. Weinstein. 1976. Tumor promoter induces plasminogen activator. *Nature* (*Lond.*). 259:232–233.
6. Diamond, L., S. O'Brian, L. Donaldson, and Y. Schimizu. 1974. Growth stimulation of human diploid fibroblasts by the tumor promoter 12-O-tetradecanoyl-phorbol-13-acetate. *Int. J. Cancer.* 13:721–730.
7. Yuspa, S. H., U. Lichti, T. Ben, E. Patterson, H. Hennings, T. Slaga, N. Colburn, and W. Klesey. 1976. Phorbol esters stimulate DNA synthesis and ornithine decarboxylase activity in mouse epidermal cultures. *Nature* (*Lond.*). 263:402–404.
8. Driedger, P. E., and P. M. Blumberg. 1980. Specific binding of phorbol ester tumor promoters. *Proc. Natl. Acad. Sci. USA.* 77:567–571.
9. Shoyab, M., and G. J. Todaro. 1980. Specific high affinity cell membrane receptors for biologically active phorbol and ingenol esters. *Nature* (*Lond.*). 288:451–455.
10. Niedel, J. E., L. J. Kuhn, and G. R. Vanderbank. 1983. Phorbol diester receptor copurifies with protein kinase C. *Proc. Natl. Acad. Sci. USA.* 80:36–40.
11. Leach, K. L., M. L. James, and P. M. Blumberg. 1983. Characterization of a specific phorbol aster aporeceptor in mouse brain cytosol. *Proc. Natl. Acad. Sci. USA.* 80:4208–4212.
12. Kikkawa, U., Y. Takai, Y. Tanaka, R. Miyake, and Y. Nishizuka. 1983. *J. Biol. Chem.* 258:11442–11445.
13. Laszlo, A., K. Radke, S. Chin, and M. J. Bissel. 1981. Tumor promoters alter gene expression and protein phosphorylation in avian cells in culture. *Proc. Natl. Acad. Sci. USA.* 78:6241–6245.
14. Feuerstein, N., and H. L. Cooper. 1983. Rapid protein phosphorylation induced by phorbol ester in HL-60 cells. *J. Biol. Chem.* 258:10786–10793.
15. Rozengurt, E., M. Rodriguez-Pena, and K. A. Smith. Phorbol esters, phospholipase C, and growth factors rapidly stimulate the phosphorylation of a M_r 80,000 protein in intact quescent 3T3 cells. *Proc. Natl. Acad. Sci. USA.* 80:7244–7248.
16. Gilmore, T., and G. S. Martin. 1983. Phorbol ester and diacylglycerol induce protein

phosphorylation at tyrosine. *Nature (Lond.)*. 306:487–498.
17. Quigley, J. P. 1979. Phorbol ester-induced morphological changes in transformed chick fibroblasts: evidence for direct catalytic involvement of plasminogen activator. *Cell*. 17:131–141.
18. Rifkin, D. B., R. M. Crowe, and R. Pollak. 1979. Tumor promoters induce changes in the chick embryo fibroblast cytoskeleton. *Cell*. 18:361–368.
19. Boreiko, C., S. Mondal, K. S. Narajan, and C. Heidelberger. 1980. Effect of 12-O-tetradecanoylphorbol-13-acetate on the morphology and growth of C3H/10T1/2 mouse embryo cells. *Cancer Res*. 40:4709–4716.
20. Ojakian, G. K. 1981. Tumor promoter-induced changes in the permeability of epithelial cell tight junctions. *Cell* 23:95–103.
21. Nagle, D. S., and P. M. Blumberg. 1980. Activity of phorbol ester tumor promoters on enucleated swiss 3T3 cells. *Cancer Res*. 40:1066–1072.
22. Schliwa, M., and J. van Blerkom. 1981. Structural interaction of cytoskeletal components. *J. Cell Biol*. 90:222–235.
23. Schliwa, M., U. Euteneuer, J. C. Bulinski, and J. G. Izant. 1981. Calcium lability of cytoplasmic microtubules and its modulation by microtubule-associated proteins. *Proc. Natl. Acad. Sci. USA*. 78:1037–1041.
24. Weber, K., P. C. Rathke, and M. Osborn. 1978. Cytoplasmic microtubular images in glutaraldehyde-fixed tissue culture cells by electron microscopy and by immunofluorescence microscopy. *Proc. Natl. Acad. Sci. USA*. 75:1820–1824.
25. Wieland, T. 1977. Modification of actin by phallotoxins. *Naturwissenschaften*. 64:303–309.
26. Geiger, B. 1979. A 130k protein from chicken gizzard: its localization at the termini of microfilament bundles in cultured chicken cells. *Cell* 18:193–205.
27. Burridge, K., and J. R. Feramisco. 1980. Microinjection and localization of a 130k protein in living fibroblasts: a relationship to actin and fibronectin. *Cell*. 19:587–595.
28. Shriver, K., and L. Rohrschneider. 1981. Organization of $pp60^{src}$ and selected cytoskeletal proteins within adhesion plaques and junctions of Rous sarcoma virus-transformed cell. *J. Cell Biol*. 89:525–535.
29. Avnur, Z., and B. Geiger. 1981. Substrate-attached membranes of culture cells. Isolation and characterization of ventral cell membranes and the associated cytoskeleton. *J. Mol. Biol*. 153:361–379.
30. Pryzwansky, K. B., M. Schliwa, and K. R. Porter. 1983. Comparison of the three-dimensional organization of unextracted and Triton-extracted human neutrophilic polymorphonuclear leukocytes. *Eur. J. Cell Biol*. 30:112–125.
31. Schiff, P. B., and S. B. Horowitz. 1980. Taxol stabilizes microtubules in mouse fibroblast cells. *Proc. Natl. Acad. Sci. USA*. 77:1561–1565.
32. De Brabander, M., G. Geuens, R. Nuydens, R. Willebrords, and J. de Mey. 1981. Taxol induces the assembly of free microtubules in living cells and blocks the organizing capacity of the centrosome and kinetochores. *Proc. Natl. Acad. Sci. USA*. 78:5608–5612.
33. Green, K. J., and R. D. Goldman. 1983. The effects of taxol on cytoskeletal components in cultured fibroblasts and epithelial cells. *Cell Motility*. 3:283–30[illegible].
34. Hynes, R. O. 1981. Relationships between fibronectin and the cytoskeleton. *Cell Surf. Rev*. 7:97–156.
35. Chen, L. B., N. Maitland, P. H. Gallimore, and J. K. McDougall. 1977. Detection of the external transformation-sensitive protein on some epithelial cells. *Exp. Cell Res*. 106:39–46.
36. Rochette-Egly, C., and M. Castagna. 1979. Tumor promoting phorbol ester inhibits the cyclic AMP response of rat embryo fibroblasts to chatecholamines and prostaglandin E_1. *FEBS (Fed. Eur. Biochem. Soc.) Lett*. 103:38–42.
37. Ludwig, K. W., and R. M. Niles. 1980. Suppression of cyclic AMP dependent protein kinase activity in murine melanoma cells by 12-O-tetradecanoylphorbol-13-acetate. *Biochem. Biophys. Res. Commun*. 95:296–303.
38. Marks, F., G. Furstenberger, and E. Kownatzki. 1981. Prostaglandin E-mediated mitogen stimulation of mouse epidermis in vivo by divalent cation ionophore A23187 and by tumor promoter TPA. *Cancer Res*. 41:696–702.
39. Gunther, G. R. 1981. Effect of 12-O-tetradecanoylphorbol-13-acetate on Ca^{++} efflux and protein discharge in pancreatic acini. *J. Biol. Chem*. 256:12040–12045.
40. Brostrom, M., C. O. Brostrom, L. A. Brotman, C. Lee, D. J. Wolff, and H. M. Geller. 1982. Alterations of glial tumor cell Ca^{++} metabolism and Ca^{++}-dependent cAMP accumulation by phorbol myristate acetate. *J. Biol. Chem*. 257:6758–6765.
41. Mastro, A. M., and M. C. Smith. 1983. Calcium-dependent activation of lymphocytes by ionophore, A23187, and a phorbol ester tumor promoter. *J. Cell. Physiol*. 116:51–56.
42. Froscio, M., G. R. Guy, and A. W. Murray. 1981. Calmodulin inhibitors modify cell surface changes triggered by a tumor promoter. *Biochem. Biophys. Res. Commun*. 98:829–835.
43. Kwong, C. H., and G. C. Mueller. 1982. Antagonism of Con A-capping in phorbol ester activated lymphocytes by calmodulin inhibitors and certain amino acid esters. *Cancer Res*. 42:2115–2120.
44. Cheung, W. Y. 1979. Calmodulin plays a pivotal role in cellular regulation. *Science (Wash. DC)*. 207:19–27.
45. Van Belle, H. 1981. R24571: a potent inhibitor of calmodulin activated enzymes. *Cell Calcium*. 2:483–494.
46. Weber, K., P. Rathke, and M. Osborn. 1976. Distribution of actin and tubulin in cells and glycerinated cell models after treatment with cytochalasin B. *Exp. Cell Res*. 102:285–297.
47. Godman, G., and A. Miranda. 1978. Cellular contractility and the visible effects of cytochalasin. *In* Cytochalasins: Biochemical and Cell Biological Aspects. S. Tannenbaum, editor. Elsevier/North Holland, Amsterdam. 277–429.
48. Schliwa, M. 1982. Action of cytochalasin D on cytoskeletal networks. *J. Cell Biol*. 92:79–91.
49. Crutchley, D. J., L. B. Conanan, and J. R. Maynard. 1980. Induction of plasminogen activator and prostaglandin biosynthesis in HeLa cells by 12-O-tetradecanoyl-phorbol-13-acetate. *Cancer Res*. 40:849–852.
50. Cohen, R., M. Pacifici, N. Rubenstein, J. Biehl, and H. Holtzer. 1977. Effect of a tumor promoter in myogenesis. *Nature (Lond.)*. 266:538–540.
51. Hiwasa, T., S. Fujimura, and S. Sakiyama. 1982. Tumor promoters increase the synthesis of a 32,000-dalton protein. *Proc. Natl. Acad. Sci. USA*. 79:1800–1804.
52. Laszlo, A., and M. Bissel. 1983. TPA induces simultaneous alterations in the synthesis and organization of vimentin. *Exp. Cell Res*. 148:221–234.
53. David-Pfeuty, T., and S. J. Singer. 1980. Altered distributions of the cytoskeletal proteins vinculin and α-actinin in cultured fibroblasts transformed by Rous sarcoma virus. *Proc. Natl. Acad. Sci. USA*. 77:6687–6691.
54. Nigg, E. A., B. M. Sefton, T. Hunter, G. Walter, and S. J. Singer. 1982. Immunofluorescent localization of the transforming protein of Rous sarcoma virus with antibodies against a synthetic src peptide. *Proc. Natl. Acad. Sci. USA*. 79:5322–5326.
55. Kartenbeck, J., E. Schmid, W. W. Franke, and B. Geiger. 1982. Different modes of internalization of proteins associated with adherens junctions and desmosomes. *EMBO (Eur. Mol. Biol. Organ.) J*. 1:725–732.
56. Stanka, P. 1973. Uber ein intrazellulares Desmosom einer Haarwurzelzelle. *Z. Zellforsch. Mikrosk. Anat*. 141:299–300.
57. Schliwa, M. 1974. Asymmetrische und intracytoplasmatische Desmosomen in Fischepidermiszellen. *Cytobiologie*. 9:221–227.
58. Burridge, K., and J. R. Feramisco. 1982. α-Actinin and vinculin from non-muscle cells: calcium-sensitive interactions with actin. *Cold Spring Harbor Symp. Quant. Biol*. 46:587–597.
59. Wilkens, J. A., and S. Lin. 1982. High affinity interaction of vinculin with actin filaments in vitro. *Cell*. 28:83–90.
60. Jockusch, B. M., and G. Isenberg. 1981. Interaction of α-actinin and vinculin with actin: opposite effects on filament network formation. *Proc. Natl. Acad. Sci. USA*. 78:3005–3009.
61. Lehtonen, E., V. P. Lehto, R. A. Badley, and I. Virtanen. 1983. Formation of vinculin plaques precedes other cytoskeletal changes during retinoic acid-induced teratocarcinoma cell differentiation. *Exp. Cell Res*. 144:191–197.
62. Geiger, B. 1982. Involvement of vinculin in contact-induced cytoskeletal interactions. *Cold Spring Harbor Symp. Quant. Biol*. 46:671–682.
63. Werth, D. K., J. E. Niedel, and I. Pastan. 1983. Vinculin, a cytoskeletal substrate for protein kinase C. *J. Biol. Chem*. 258:11423–11426.
64. Sefton, B. M., T. Hunter, E. H. Ball, and S. J. Singer. 1981. Vinculin: a cytoskeletal target of the transforming protein of Rous sarcoma virus. *Cell*. 24:165–174.
65. Rohrschneider, L., and M. J. Rosok. 1983. Transformation parameters and $pp60^{src}$ localization in cells infected with partial transformation mutants of Rous sarcoma virus. *Mol. Cell Biol*. 3:731–746.
66. Rosok, M. J., and L. Rohrschneider. 1983. Increased phosphorylation of vinculin tyrosine does not occur during the release of stress fibers before mitosis in animal cells. *Mol. Cell. Biol*. 3:475–479.
67. Sando, J. J., and M. C. Young. 1983. Identification of high affinity phorbol ester receptor in cytosol of EL4 thyoma cells: requirement for calcium, magnesium, and phospholipids. *Proc. Natl. Acad. Sci. USA*. 80:2642–2646.
68. Nishizuka, Y. 1983. Phospholipid degradation and signal translation for protein phosphorylation. *Trends Biochem. Sci*. 8:13–16.